Sensors and Actuators B 269 (2018) 210–222

Contents lists available at ScienceDirect

Sensors and Actuators B: Chemical

journal homepage: www.elsevier.com/locate/snb

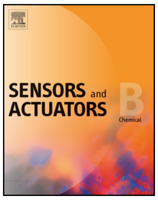

Nanosheet-assembled NiO microspheres modified by Sn^{2+} ions isovalent interstitial doping for xylene gas sensors

Hongyu Gao, Qi Yu, Sufang Zhang, Tianshuang Wang, Peng Sun*, Huiying Lu, Fangmeng Liu, Xu Yan, Fengmin Liu, Xishuang Liang, Yuan Gao, Geyu Lu*

State Key Laboratory on Integrated Optoelectronics, College of Electronic Science and Engineering, Jilin University,2699 Qianjin Street, Changchun 130012, China

ARTICLE INFO

Article history:
Received 11 January 2018
Received in revised form 8 April 2018
Accepted 26 April 2018
Available online 30 April 2018

Keywords:
NiO microspheres
Isovalent interstitial doping
Defects
Anti-humidity properties
Xylene sensor

ABSTRACT

Hierarchical NiO nanomaterials doped by 0.5, 1.0, 1.5 and 2.0 at% Sn^{2+} ions were synthesized through a facial hydrothermal route. The isovalent Sn^{2+} ions were selected as dopants and occupied the interstitial spaces of NiO lattice. Such obtained NiO specimens were characterized by X-ray powder diffraction (XRD), scanning electron microscopy (SEM), transmission electron microscopy (TEM), X-ray photoelectron spectroscopy (XPS) etc. and used as sensing materials for gas sensors. The comparative sensing property tests among these Sn^{2+} doped NiO sensors demonstrated that 1.5 at% Sn^{2+}-NiO microspheres showed the highest response (~25.2 ± 10%) to 200 ppm xylene, which was about 14-fold higher than that of the pure NiO. Moreover, the humidity-independent performance of the 1.5 at% Sn^{2+}-NiO sample was excellent, such as low detection limit (1.1-500 ppb) and good selectivity toward xylene at high relative humidity (90% RH). The gas sensing mechanisms for the improved sensing performance were also discussed.

1. Introduction

In order to meet the increasing needs of detecting and monitoring the polluted gases, gas sensors based on oxide semiconductor stand out, because of their fascinating merits such as low cost, easy integration, controllable preparation and so on [1,2]. The dominating part of this kind of sensor ought to be the sensing material belonging to n-type or p-type oxide semiconductors roughly. In the past few decades, more researches on the n-type semiconductor gas sensors have been done compared with that on the p-type semiconductor gas sensors [3]. The sensors fabricated from some representative n-type oxide semiconductors such as SnO_2, ZnO, In_2O_3 and α-Fe_2O_3 showed rapid and reliable detection of some typical volatile organic compounds (VOCs) and other gases such as ethanol, acetone, formaldehyde, NH_3, NO_x etc. [4–7]. Actually, the utility of n-type oxide semiconductors is still limited to a few gases, owing to their low selectivity and significant humidity interference [4,8,9]. Therefore, it is needed to find alternative materials which can overcome these problems and give better gas sensing performance at moderate temperatures. As the alternatives, p-type oxide semiconductors such as NiO, Co_3O_4, CuO, and Cr_2O_3 are some promising materials with good sensing performance toward xylene, C_2H_5OH, acetone, NH_3, H_2, CO, and H_2S gases [3,8,10–13]. Similar discussions could be applied to xylene gas sensors. Some works about xylene gas sensors (shown in Table 3) have been reported in recent years [14–26], and the sensing materials were mainly WO_3, MoO_3, α-Fe_2O_3, TiO_2, ZnO, Cr_2O_3, Co_3O_4, NiO materials modified by various methods (e.g. noble metal loading, hybrid materials formation with hetero-junctions and aliovalent metal ions doping). Clearly, comprehensive test and analysis about humidity interference were seldom discussed in the reported xylene sensors, as water vapor was always an unfavorable factor for gas sensitivity. In addition, though high gas responses were achieved sometimes, issues still existing for the xylene gas sensors, such as poor selectivity and low response-recovery speed [3,13,19,21].

Generally speaking, the gas sensing properties of n-type oxide semiconductors are better than that of p-type oxide semiconductors as a consequence of the equation$S_P = \sqrt{S_N}$, where S_P and S_N are the gas sensitivities of the p-type and n-type oxide semiconductors with same morphologies [27]. This equation clearly demonstrates the challenge of designing high-performance gas sensors using p-type oxide semiconductors. Nickel oxide, as a representative p-type oxide semiconductor with NaCl-type crystal structure [28], is broadly employed in various areas including catalysis [29,30], super capacitors [31,32], lithium ion batteries [33,34],

---

* Corresponding authors.
E-mail addresses: pengsun@jlu.edu.cn (P. Sun), lugy@jlu.edu.cn (G. Lu).

https://doi.org/10.1016/j.snb.2018.04.161
0925-4005/

magnetic materials [35,36], electrochromic display devices [37,38], gas sensors [39,40] etc. owing to its superior chemical and electrical properties. As for its application in gas sensors, most literatures reported those well-modified NiO hierarchical nanostructures as sensing materials, because pristine NiO with no improved modifications showed low gas responses and could not transfer the chemical signals into significant electrical signals [40–44]. Fortunately, NiO exhibits superior catalytic oxidation activity [45,46] in the reactions with the volatile organic compounds (VOCs). Moreover, the chemisorbed oxygen amount on NiO surface is higher than that of other metal oxides [47]. These advantages make the modification research of NiO sensing materials meaningful and distinctive.

Through investigation of substantial literatures, at present, reported researches on the gas sensing materials are mainly focused on the preparation of novel hierarchical structures and improvement with different modification approaches. There are three main types of modification methods [3,48], including noble metal catalysts loading, hybrid materials formation with heterojunctions and aliovalent metal ions doping. As far as NiO is concerned, catalyst loading refers that loading some noble metals or metal oxide particles (such as Au, Pt, PdO) with minimal sizes (usually <10 nm) on the surface of NiO nanomaterials [49–51]. The excellent catalytic activities and the energy-band changes caused by the “Schottky barrier” contribute to the enhanced sensing properties. The formation of the heterostructure means that growing another kind of oxide semiconductor on the basis of NiO nanostructure. The formed heterojunctions (p-n or p-p) will change the material morphology, surface activity and band structure, thereby improving the sensing performance [52–54]. Cation doping of aliovalent metal ions is a modification method that incorporating the metal ions of different valence with Ni^{2+} into the NiO lattice, occupying the Ni^{2+} sites and introducing the impurity level [26,42,55–58]. This doping will make changes in crystal structure, grain size, carrier concentration and oxygen distribution, thus improving the sensing properties of NiO based gas sensors.

On the basis of above discussion, poor selectivity and obvious humidity interference were main and universal problems for gas sensors. The main purpose of this work was to show a less-used modification method and the design of xylene sensor having enhanced properties with good selectivity and anti-humidity performance. Thus in this paper, a novel modification method of isovalent interstitial doping was used to improve the NiO sensing performance. We successfully incorporated Sn^{2+} ions into NiO interstitial void and obtained nanosheet-assembled NiO microspheres. Gas sensors were fabricated from the as-obtained specimens, and their sensing performances were tested with a static test system. The results demonstrated that 1.5 at% Sn^{2+} doped NiO showed superior xylene sensing properties with high sensitivity, low detection limit, good selectivity and anti-humidity properties, indicating its potential application as a sensing material for a superior xylene sensor.

2. Experimental

2.1. Synthesis of the nanosheet-assembled pure and Sn^{2+} doped NiO

All involved chemicals were analytical grade reagents and directly used without further purification. A hydrothermal route was adopted to synthesize the pure and Sn^{2+} doped NiO hierarchical nanostructures. In the experiment, 0.475 g (2 mmol) of $NiCl_2 \cdot 6H_2O$ was measured with an electronic balance and dissolved into 30 mL of deionized water in a beaker under continuous magnetic stirring at room temperature. Then various amounts (0, 0.01, 0.02, 0.03 and 0.04 mmol) of $SnCl_2 \cdot 2H_2O$ (Sn/Ni = 0, 0.5, 1, 1.5, and 2 at%, respectively) and 0.281 g of hexamethylenetetramine (HMT) were added sequentially into the beaker to form a clear mixture solution. After five minutes magnetic stirring, 2 mL of ethanolamine was dropwise added into the mixed solution. Next, after vigorous stirring for 15 min at room temperature, the final solution was transferred into a 45 mL Teflon-lined stainless steel autoclave and reacted at a constant temperature of 160 °C for 12 h in the hot oven. When the time was over and temperature decreased to room temperature naturally, the resulting precipitate was separated by centrifugation and rinsed with ethanol and deionized water alternately several times. Then put the centrifuged precipitate in the oven drying at 80 °C overnight. At last, the pure and Sn^{2+} doped NiO with different molar ratios samples were finally obtained after calcining at 400 °C for 2 h in the muffle furnace with a heating rate of 5 °C/min.

2.2. Characterization

The crystalline characteristics of the pure and Sn^{2+} doped NiO were collected from the X-ray powder diffraction (XRD) analysis using a Rigaku D/Max-2550 diffractometer with Cu Kα radiation ($\lambda = 1.541$ Å; 40 kV, 350 mA) in the 2θ range from 20° to 80° with a step rate of 10°/min. In the XRD test, obtained samples were supported on the glass substrate separately and measured in reflection mode. Morphological and structural characteristics were analyzed by field emission scanning electron microscopy (FESEM) with a JSM-7500F (JEOL) microscope operating at an accelerating voltage of 15 kV and by transmission electron microscopy (TEM) and high-resolution TEM with a JEM-2200FS (JEOL) instrument operating at 200 kV. The analyses of energy dispersive X-ray spectroscopic (EDS) were obtained with the help of TEM attachment. The Brunauer-Emmett-Teller (BET) surface area and other textural parameters were tested by nitrogen adsorption-desorption on Micromeritics Gemini VII apparatus and chemical element analyses were obtained from X-ray photoelectron spectroscopy (XPS) measurements with a source of Mg-Kα X-ray (1253.6 eV Specs XR50).

2.3. Fabrication and measurement of gas sensor

The gas sensors were fabricated from the obtained specimens and the schematic structure of the sensor is shown in Fig. S1. First, the as-synthesized powder and deionized water were mixed together to form a slurry and then, the slurry was coated uniformly on the surface of the ceramic tube (external diameter: 1.2 mm, internal diameter: 0.8 mm and length: 4 mm), where a pair of gold electrodes with four Pt wires had been installed. After drying in air for 30 min, the well-coated tube was sintered at 400 °C for 2 h in the muffle furnace with a heating rate of 5 °C/min. And after that, a Ni-Cr alloy coil heater was inserted through the tube controlling the working temperature via the flowing current. Finally, the sensor was welded on a hexagon socket and tested through a static test system after one-week ageing with an aging current about 100 mA. Our static test system can record real-time sensor resistance, it is mainly made up of four parts: A constant-current power (Gwinstek GPD-3303S) providing different working temperatures to the sensors; An airtight chamber separating out a close space, where the gas can be changed by an air pump; A Fluke 8846a (Fluke Co.) recording the resistance of the sensors; A computer which can display and save the test data. In the test, the sensor was placed separately in the airtight chambers (1 L in volume) filled with pristine air and a given quantity of the target gases (injected into the chamber using a microsyringe) to measure the sensing properties. All the changes of sensor resistances (except for the humid interference test) were collected under a laboratory conditions (50% RH, 20 °C), which was controlled and maintained by a big air con-